Scholar Publishing Group
International Journal of Engineering Technology and Construction
https://doi.org/10.38007/IJETC.2022.030101
ISSN 2789-7176 Vol. 3, Issue 1: 1-16

TBM Construction Tunnel Forward-to-cross-hole Radar Transmission Imaging Leading Potential Rockburst Geological Forecast Safety Monitoring System and Method

Qiwen Zhou[1], Runzhi Jia[1*], Zhansheng Lin[2] and Fucai Pei[2]

[1]*China National Chemical Communications Construction Group Co., Ltd, China*

[2]*Shandong Luqiao Group Co., Ltd, Jinan, Shandong, China*

31390800@qq.com

[*]*corresponding author*

Keywords: Tunneling Boring Machine (TBM), Tunnel Geological Advance Prediction, Rock Burst Prediction, Intensity Stress Ratio

Abstract: At present, the technology of tunnel geological engineering is not mature enough, and there are many deficiencies in the tendency index of rock burst, which need to be improved in construction safety. The purpose of this paper is to study the geological safety monitoring system of TBM construction tunnel forward-to-cross-hole radar transmission imaging advanced potential rock burst. This paper combines the tunnel geology super Pre-prediction is a specific application, the pulse system of ground penetrating radar launch and acquisition system is designed. The system synchronous control module with single chip microcomputer as the core device is designed to produce square wave signal with adjustable frequency, which provides synchronous trigger signal for the avalanche pulse generation circuit and data acquisition module. The experimental data show that the system can realize the functions of producing avalanche pulse signal, sending and receiving synchronously and displaying in real time. resulting in an increase in the safety detection coefficient of about 80%. The experimental data show that the development of forward trans-hole radar transmission imaging is very important for the development of geophysical instruments It is of great significance to establish the safety monitoring system of TBM construction tunnel forward-to-cross-hole radar transmission imaging leading potential rock burst geological forecast.

1. Introduction

In recent years, with the development of China's economic construction, the construction of

highway, railway and subway tunnels has increased greatly, and in the construction of tunnels, due to the unclear geological structure in front of the face of the face, they often encounter geological disasters such as landslides, roof fall, water gushing, mud outburst and rock burst in the construction [1-3]. Due to the lack of reliable geological advance forecast in the construction process, the potential geological hazard may become a geological disaster, which will cause the increase of construction period, the increase of capital cost and the damage of machinery and equipment, the casualties of personnel and the difficulty of subsequent construction. Great loss of personnel and property. The factors causing the disaster in the excavation of the tunnel are various, such as the reasons of geological structure characteristics, such as groundwater, toxic gas, flammable gas, high altitude temperature, rock burst, etc., but also the reasons of people's insufficient understanding of geological structure characteristics and improper construction methods, such as collapse, roof fall and so on. Therefore, it is very important to forecast the surrounding rock status, fault, fracture zone and water content in the tunneling process .

F.C. Frischnecht in the book of electromagnetic law has proposed that for a physical simulation (or scale model simulation) a geological model should be reproduced in a laboratory at some scale (usually between 1:120 and 1:106). In people's understanding of the physical and chemical properties of strata and the structural state of rock mass itself, it is necessary to obtain the basis of qualitative and quantitative analysis through a variety of exploration and test means [4-6]. At present, the main geophysical exploration methods for advance prediction in tunnel construction at home and abroad are seismic wave reflection method and low frequency GPR method. Each of the above two methods has its own advantages and disadvantages. The shooting method is characterized by long distance, reliable and intuitive detection, but the detection speed is slow, the cost is high, the resolution is low, and the project progress is affected. The GPR method is characterized by nondestructive detection, low cost, high efficiency and high resolution, but the detection distance is very close [7-8]. for shallow, high-resolution detection in the ground penetrating radar has advantages. The ground penetrating radar method not only has extensive and important application value in tunnel geological advance detection, but also its application scope has covered archaeology, mineral resources exploration, geotechnical engineering investigation, engineering quality inspection, building engineering structure inspection and military exploration and other related fields [9-11]. Ground penetrating radar the wide application of technology will certainly reduce the incidence of construction accidents, improve construction efficiency, shorten construction cycle, avoid accident losses, save investment, and thus bring great social and economic benefits [12].

D. Moher has proposed a whole set of construction techniques for tunnel construction in rock burst geology. Rock burst is a kind of sudden disaster which is easy to occur in deep-buried brittle, high-strength hard rock and structural development tunnel. The occurrence of rock burst directly threatens the construction process, how to reasonably and timely predict and forecast the rock burst condition in the construction stage, and it is very important and necessary to adjust the support design, ensure the safety of the construction personnel and arrange the construction schedule reasonably [13-14]. Single Index Rock The blasting evaluation is based on a particular or multiple rock burst engineering examples and the corresponding test data, and has its limitations, that is, the single index evaluation information is relatively single, the huge variability of the rock mass itself and the complexity of the project itself often lead to the deviation of the evaluation results: most of the single index parameters are based on the uniaxial compression test of rock, only considering the uniaxial rock physical mechanical index simply, ignoring the quality characteristics of the engineering rock mass and the construction characteristics, so the rock burst possibility may be wrongly evaluated [15-16].

The rockburst evaluation can be divided into the rockburst potential trend assessment (long-term,

regional) in the engineering research stage and the rockburst prediction and forecast in the construction stage (short-term, timely)[17]. The long-term regional evaluation gives the macroscopic understanding of the existence or not of rock burst and the grade of strength, which is of guiding significance to the stage of engineering research [18]. The short-term and timely forecast gives the concrete detailed rock burst forecast for the local excavation section, which is of practical significance to the construction stage of the project [19-21]. The above-mentioned single index discrimination or parallel comprehensive multi-index discrimination are only macroscopic evaluation of the risk of rock burst in the research stage [22]. Rockbursts in the tunnel construction phase The measurement is relatively local and specific, and more difficult, with the change of excavation conditions, the factors to be considered are more diverse and rich. For the rock burst prediction in the construction stage, the real-time on-line monitoring based on acoustic emission, microseismic, acoustic wave, electromagnetic and other technologies [23-24] has achieved fruitful work, but the investment cost is high, and the application effect is sometimes not very ideal because of the complexity of the geological environment of the field engineering and the interference of the operation of the construction machinery due to the performance and technical constraints of the monitoring system [25]. How to consider the characteristics of rock mass, stress state and geological structure in the construction stage based on the field test of the project The establishment of a quick, simple and economical quantitative index of rock burst in the construction stage is a difficult problem to be solved, and it is also a technical discussion on the comprehensive quantitative expression of rock burst prediction problem [26-28].

2. Proposed Method

2.1. Composition of Forward Cross-Hole Radar System

The machine control system is composed of avalanche pulse generation circuit, which can produce control pulse signal of different frequency according to the instruction of upper computer, as the trigger signal of avalanche pulse generation circuit, and also as the synchronous signal of data acquisition module. An avalanche pulse signal with a duration of nanoseconds is generated when the avalanche transistor breaks through. The signal is transmitted to the transmitting antenna through a coaxial cable, and the electromagnetic wave signal is radiated underground by the transmitting antenna, and the echo signal is received by the antenna after reflection by the target body. The data acquisition module is used to collect the data and transmit the data to the upper computer through the bus. Based on the two-dimensional echo waveform of time domain, the data processing and interpretation of echo signal are used to analyze the location of underground target body.

A forward cross-hole radar system is an electromagnetic technique for locating objects or interfaces that are not visible underground or within an object. Its working principle is that the high frequency electromagnetic wave is in the form of wide band pulse, which is directed into the ground through the transmitting antenna, and then returned to the ground through the reflection of the underground formation or the target body with electrical difference, which is received by the receiving antenna. When the electromagnetic wave propagates in the medium, its path, electromagnetic field intensity and waveform will change with the electromagnetic characteristics and geometric shape of the medium through which it passes, so the structure or buried object of the underground can be judged by analyzing and processing the received signal. The working principle formula of GPR is shown below. According to the launch letter The time difference between the signal and the received signal, and the speed of electromagnetic wave propagation underground, can calculate the depth of the target body.

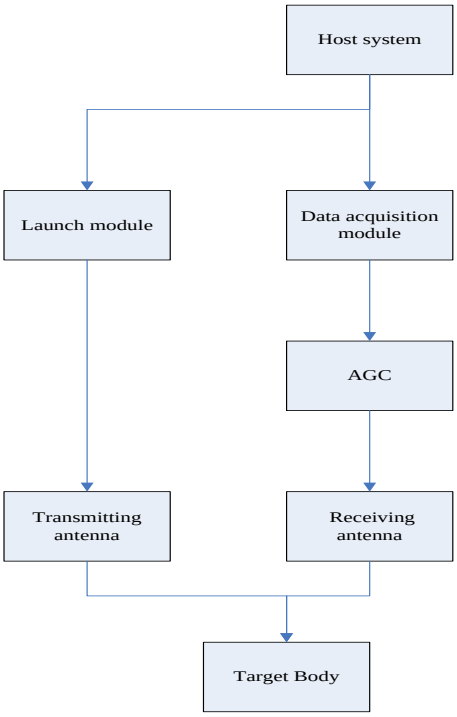

Figure 1. Radar launch and receive system

$$D = V \bullet \Delta T / 2 \tag{1}$$

Because the composition of underground strata is complex and generally contains more moisture, in order to improve the penetration ability, the radar wave with lower frequency is generally used, the higher the frequency of electromagnetic wave is, the weaker its penetration ability is, but the higher the resolution is. the amplitude change of the reflected and transmitted waves of the gpr is related to the polarization characteristics of the microwave. in parallel polarization, when the incident angle is equal to the bush angle is shown below.

$$\theta_i = \theta_b = \sin' \sqrt{\frac{\varepsilon_2}{\varepsilon_1 + \varepsilon_2}} \tag{2}$$

The size of the smallest anomaly that GPR can distinguish in the horizontal direction is called horizontal resolution. The horizontal resolution of the radar profile can usually be illustrated by the band, which is the interference principle of the wave, and the amplitude is strengthened by the phase length interference in the first band. in the second zone for the elimination of interference, the amplitude is weakened. The third band (phase length), the fourth band (elimination). In engineering practice, the diameter of the first band is defined as follows when the depth of the reflection interface is much less than that of the transmitting and receiving antennas.

$$d_F = \sqrt{\frac{\lambda H}{2}} \tag{3}$$

The wavelength of the radar wavelet and H is the buried depth of the anomaly body.

The ability to distinguish between more than one reflective interface in a GPR profile is called vertical resolution. The diagram shows that the lower formula is usually used as the lower limit of the vertical resolution.

$$b = \frac{\lambda}{4} \tag{4}$$

GPR can detect the depth of the deepest object called GPR. When the radar system is selected, the gain of the system is the transmission power of the instrument, which is the background noise of the receiving system. As long as the receiver's echo signal power is greater, then the echo from the target body can be identified by the GPR system. If the radiated power of the transmitting antenna is zero, the transmitting antenna efficiency takes into account the spherical diffusion of the radiated power and the absorption of the medium, as well as the directional gain of the antenna in the incident direction, the power density of the incident wave reaching the surface of the target body is as follows As shown.

$$P_s = W_t \eta_t G_t \frac{1}{4\pi r} e \tag{5}$$

The total power of the target body scattering is equal to multiplying its scattering cross section. considering the gain of the scattering body backward and the emission and absorption of the echo, the power density of the scattering wave to the receiving antenna is shown below.

$$P_r = P_s \sigma_s G_s \frac{1}{4\pi r} e \tag{6}$$

The power received by the receiving antenna depends on its effective receiving area and directional gain. the final receiving antenna receiving power is shown below.

$$W_r = W_r \eta_t \eta_r G_t G_r A_r \frac{1}{16\pi r} e \tag{7}$$

Taking into account the above non-uniform periodic sampling method, the state space model (2) can be discretized into the following lifting transfer function model using the lifting technique:

$$y(kT + t_i) = \frac{1}{\alpha(z)} \sum_{j=1}^{r} \beta_{ij}(z) \bar{u}(kT + t_{j-1}) + v(kT + t_i) \tag{8}$$

In the formula:

$$\alpha(z) = 1 + \alpha_1 z^{-1} + \alpha_2 z^{-2} + \ldots + \alpha_n z^{-n} \tag{9}$$

$$\beta_{ij}(z) = \beta_{ij}^0 + \beta_{ij}^1 z^{-1} + \beta_{ij}^2 z^{-2} + \ldots + \beta_{ij}^n z^{-n} \tag{10}$$

2.2. Hardware Design of Acquisition System

The main components of the GPR data acquisition system are the receiving antenna, the circuit and the data acquisition module. In order to ensure that the system can collect data effectively, the signal conditioning circuit should be added to the input of the data acquisition system, so that the output signal can be in a suitable range, so that the acquisition module cannot be quantified because the input signal is too small, and the acquisition module is saturated because the output signal is too large. Because the spectrum of the received signal is wide, if the data is collected in real time If so, the circuit should have sufficient bandwidth, and the data acquisition module should have sufficient bandwidth and at least four times the maximum frequency of the input signal sampling rate. Foreign equipment usually achieves sufficient bandwidth and high real-time sampling rate. However,

because of import restrictions, it is often difficult to buy high-performance acquisition boards, even if they are available at a very expensive price. For example, the real-time sampling rate card for the bandwidth that the group originally planned to purchase.

Because the performance index of domestic devices has a certain distance from abroad, it also limits the development of high-performance geological instruments and equipments in China. For the acquisition of high-frequency signals, the principle of equivalent sampling is usually adopted in China, that is, the sampling gate is controlled by accurate step delay to collect echo signals in different periods, the signal is widened by the peak holding circuit, the low speed is used to quantify, and the signal of broadening in time domain is displayed on the upper computer. However, the efficiency of this method is relatively low, and it often needs the signal of multiple signal cycles to complete one signal acquisition. Considering the frequency of the antenna center by geological advance detection in the tunnel After the request, the design index of the antenna system is set to the center frequency. Because the research object in the initial stage of design is mainly direct wave signal, the data acquisition module can meet the requirement of signal acquisition. According to the characteristics of the antenna, the center frequency of the antenna is zero, and the direct waveform of the receiving antenna with a distance of one meter is measured by oscilloscope.

2.3. Radar Antenna Design

Antenna is one of the most important components of GPR transmitting and receiving system. There are many kinds of antennas in GPR system, such as horizontal rod-like, plate-like dipole antenna, bow-tie antenna, horn antenna, antenna, antenna, antenna, antenna, cone-coil antenna, index antenna and so on. There are many applications of horizontal rod, plate-like dipole antenna, bow-tie antenna and horn antenna in commercial GPR system. Because the butterfly antenna is simple to make, low cost, low frequency of transmitting, and has a wide frequency band, it is one of the most widely used antennas in the GPR system. Because the main objects detected by the ground penetrating radar are consumable and heterogeneous The distribution law of homogeneous media, so its antenna is also special. According to the characteristics of the ground penetrating radar, the solution of the butterfly-shaped ultra-wideband antenna is as follows:

(1) The ground penetrating radar transmitting antenna shall be capable of radiating as much energy from electromagnetic waves as possible, i.e. the antenna shall be of high efficiency. in the process of design, the radiation efficiency of the antenna is improved by measuring the sbpd of the antenna after changing the different loading, while making the antenna a good electromagnetic open system and a good match with the transmitter and receiver.

(2) The antenna should have good directionality, and the radiation pattern of the butterfly antenna is obtained by simulation in the course of the experiment.

(3) The antenna shall have sufficient bandwidth to meet the resolution requirements for the underground media.

(4) The antenna of GPR should have strong anti-jamming capability to satisfy the application of GPR system in different complex environments.

(5) The ground penetrating radar is detected in the form of pulsed electromagnetic waves and therefore requires that the electromagnetic wave sub-wave waveforms transmitted by the ground penetrating radar antennas are regular and do not produce oscillations.The time domain waveforms and radiation patterns of the receiver and receiver are presented to match the ultra wideband antenna with the avalanche pulse generation circuit.

In the design process, the main use of the Smith circle map method to match the antenna. A Smith circle graph is a graph interwoven with many circles, which can be used correctly to obtain the matching impedance of a complex system. Using an Anli vector network analyzer to measure

the antenna's Smith circle diagram, the impedance of the antenna is obtained, and then the impedance matching network design is carried out according to the Smith circle diagram. The actual antenna size cannot be too large, the antenna cannot effectively radiate the energy is reflected in the edge of the antenna, which can make the transmitting system work unstable. The ideal history is obtained to improve the stationability of antennas mice round graph, the antenna is loaded with lumped elements. the effect of loading on antenna efficiency can be reduced by selecting the appropriate loading position. both theoretical simulation and practical debugging show that for the resistance of the absorbed power, the more energy the loading position absorbs closer to the feed point, which is due to the large current element density near the feed point. In order to take into account the efficiency of the antenna, two ψ resistors are loaded on both sides of the antenna at the end of the antenna far away from the feed point, which not only reduces the reflection but also ensures the symmetry of the antenna. By analyzing the measured impedance circle diagram, it is found that the impedance inductance of the antenna is too large, so an electricity is loaded in parallel near the feeding point sense, reducing the antenna's inductive impedance and making the antenna cannot radiate the DC component directly to the ground. The test results show that lumped load improves the standing wave performance of the antenna. Compared with the received waveform before and after loading, it can be seen that the radiation efficiency of the antenna is less affected by this loading.

2.4. Multi-model Identification Algorithm for Forward Trans-hole Radar Transmission Imaging System

Industrial systems are often multivariable, strongly coupled, nonlinear, and have broad operating conditions. especially when the nonlinear characteristics of the system are unknown, it is difficult to use the traditional nonlinear structure to describe it. although it is possible to use neural networks (nn), support vector machines (svm), and wavelet networks to identify such systems, the use of such methods is often too limited to be identified because it is often difficult to determine the structure of the model and the dimensions of the parameters. the mufti model method based on the decomposition synthesis rule provides an effective means to solve such problems. It is based on certain decomposition criteria (e.g. work range), the system is decomposed into multiple local intervals, each local interval is described by a linear model, and then the original nonlinear system solution is obtained according to the hard-switched or soft-switched criterion.

As a general model in multi-model form, the local model network (LMN) can describe the system as the sum of the product of the scheduling function and its corresponding local model. LMN model recognition mainly includes model structure recognition and model parameter recognition. Johansson, wait. firstly, the concept of local model network is proposed and its general expression is introduced. compared with the radial basis function network, the local model replaces the simple weight, so the lmn can be regarded as the generalized form of the radial basis function network. Murry Smith proposes two methods for identifying system parameters: local and global learning, and enables weighted least squares and least squares algorithms are used to determine the parameters of each local model. the local learning method reduces the dimension of the parameters to be identified, the computation amount is small, the computation speed is fast, and the robustness is strong. he number of local models is determined by using the search tree optimization algorithm, and the global model is further obtained by using the interpolation method, but it lacks the theoretical support of the stability of the algorithm. the recognition of the above multi-model systems is mostly based on offline data, so it is not suitable for online recognition, especially when the characteristics of object changes or new working conditions are generated, the adaptive changes of the model cannot be carried out. Realization. Xue Zhen Frame will be based on the local model

of many the model recognition algorithm is extended to online form, and the subtraction clustering algorithm is improved. The local model structure is adjusted according to each new data sample, the local model parameters are updated, and the adaptive ability of the model is enhanced.

As a special case of LMN, the multi-model switching method has been successfully used to solve the problems of motion target tracking, medical control, aircraft fault diagnosis and control. Starting from people's habitual thinking, we can use the mature linear system recognition theory to identify the linear model at each work point by linearizing the complex nonlinear system at each work point. in addition, the model switching method based on lnm is simple and effective, greatly reducing the computational burden, and has gradually become a powerful tool for nonlinear system identification. In the multi-model switching modeling method, in order to avoid the nonlinear optimization problem of identifying all parameters simultaneously, it is usually divided into two steps to identify the parameters: first, the relevant parameters in the scheduling function are determined by fuzzy clustering algorithm; then the local linear model parameters are determined according to the least squares or kalman filter iterative method. Using the lifting technique, the nonlinear system with inconsistent sampling data is transformed into the lifting state space, and the global description of the system is obtained by multi-model switching method. a recursive least square algorithm based on fuzzy clustering is proposed to identify the system structure and parameters and thus obtain the global model.

3. Experiments

3.1. Engineering Experiments

Relying on the Neelum-Jhelum (N-J) hydropower TBM diversion tunnel project in the area of strong tectonic movement, frequent seismic activity, more complex topographic and geological conditions, excavation of the tunnel through some continuous development of closed short fold structure (syncline, anticline), fold axial surface to NW 300°~330°. The influence of local structure is obvious, the lithologic boundary and occurrence of strata are changed greatly, the mechanism of local fault disturbance is very common, and the risk of rock burst is very great. The maximum buried depth of the hydropower diversion tunnel is nearly 2,000 m, and the lithology mainly corresponds to the Tertiary Middle Neocene Murree the hard brittle bluish-gray sandstone, brown-gray siltstone and weak fuchsia silty mudstone or argillaceous siltstone with red-brown mudstone; the compressive strength of sandstone and siltstone (natural) is 98.2-165.5 mpa, some even more than 200 mpa, which is a typical hard brittle rock. In the actual construction process, the rock burst situation is not so severe, most of them are no-weak rock burst, a few medium rock burst, the number of strong rock burst is less. Since the pile number 13500-06900 tunnel excavation process, with the increase of buried depth, there is no obvious law of ground stress, rock burst occurrence times In the area of 800m of shallow burying and 48MPa of stress, two strong rock burst occurs, the deep burying is 1700-1950m and the stress is 111.6MPa, but only several weak rock burst occurs; in the area of 1200m of buried depth and 87MPa of stress, many rock burst of different grade occur. Geological survey found that the distribution of fold structure (syncline and anticline) in this area, the lithologic boundary line and occurrence of strata are changed greatly, which indicates that the state of high-grade rock burst is not caused by the state of high-grade stress, and the criterion of rock burst is only from rock strength and state of stress. judge, not in line with the actual construction process; the occurrence of rock burst is closely related to stress state, geological structure, rock strength, lithology, surrounding rock quality, construction disturbance, etc. In the area affected by the structure, the main stress and the strength of the engineering rock mass can be controlled[29-30].

3.2. Experimental Environment

In the process of research and development of detection devices, we designed several experimental platforms and developed two different detection instruments according to different experimental platforms. According to different experimental platforms and detection instruments, we have carried out a lot of tests, and modified and improved the original design scheme according to the test effect, and adopted different optimization techniques to further improve the performance of the test instrument. The detection instrument design stage has been completed, and two kinds of instruments have been used to carry out a variety of platform tests, the effect has reached the requirements of scientific research and practical. Later, we will conduct some field tests to further observe the detection effect of the test instrument, and make corresponding modifications and finishes Good. Physical simulation is an important means to obtain electromagnetic parameters of various geological models. F.C. Frischnecht in the book of electromagnetic law has proposed that for physical simulations (or scale model simulations), geological models (usually between 1:120 and 1:106) need to be replicated in a laboratory at some scale, and the arrangement of electrodes should be miniaturized. To make the test results more accurate and reliable, we designed three experimental platforms according to the existing experimental conditions and experimental requirements. An upper diameter of 48.3 cm and a height of 40 cm were designed to idealize the flow direction of the current and obtain the desired contour map The cylinder with a diameter of 20cm and a height of 14.15cm is welded together as a model frame. The whole cylinder is made of stainless steel, and the whole structure has good electrical conductivity after bending through a lathe .The experimental instrument configuration is shown in Table 1 and Table 2.

Table 1. Experimental parameters

Parameter type	Parameter value
Cylinder number	6
Rated current	2A
Voltage	0-380VAC/240VDC
Electrical insulating material	noble metal
Insulator strength	500VAC50Hz,60s

Table 2. Configuration parameter

Parameter type	Parameter value
Insulation resistance	500Mn/500VDC
Working speed	0-250rpm
Construction(al) material	Alufer
Temperature range	-20℃-+80℃
Levels of protection	IP65

3.3. Experimental Steps

(1) Because of the large variations in the size and size of the field data of various factors of influence, it is necessary to standardize the sample data.

(2) Correlation analysis is used to describe the degree of close correlation between two variables. The two variables X and Y involved in the correlation analysis are both random variables and are equal. In statistical theory, correlation coefficients are usually used to reflect the degree of linear correlation of two variables. In a nonlinear system, to evaluate the nonlinear correlation of the two observation sequences, the concept of nonlinear correlation is introduced, defined as follows.

(3) In order to verify the performance of the model, the prediction results of the soft measurement are compared with the laboratory analysis data on the basis of the identified local model, and the sampling time trend is compared with the scatter plot.

4. Discussion

4.1. System Test Results and Analysis

(1) Changing the position of the anomaly on the section parallel to the TBM face

changing the position of the abnormal body on the cross section, with the rotation of the power supply electrode on the face of the tbm palm, the position of the abnormal body is judged by the potential cloud map. the size of the abnormal body (high resistance) under selected experimental conditions was 4 cm x 4 cm x 4 cm, which was located at the central axis of the face of the palm and passed to ac with a frequency of 0.1 Hz of 40 ma, where l =3 cm,6 cm,9 cm,12 cm,15 cm. as shown in figure 2, five potentials can be seen, the resistivity change process on the right side, and the 3d anomaly body position can be established according to the 2d cloud map. Results: When the abnormal body is far away, the presence of foreign bodies is judged by PFE; when the foreign bodies are in a closer position, the distance and position of the foreign bodies are accurately determined by the cloud map.

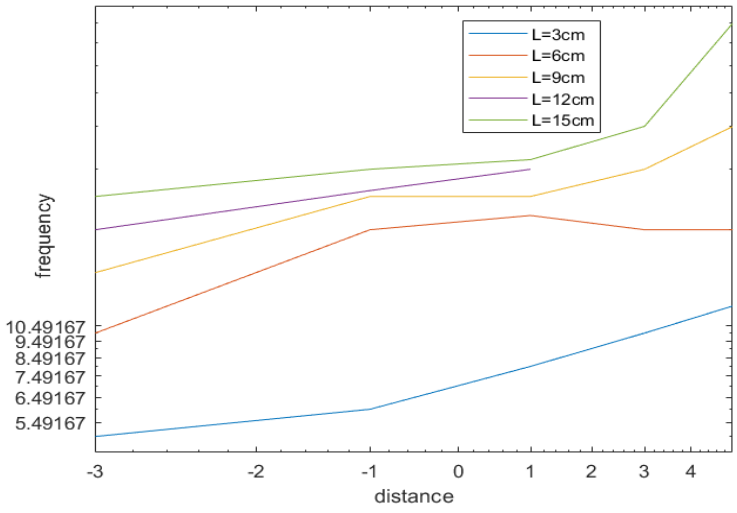

Figure 2. Depth change potential map

(2) Changing the frequency of the supply current

By changing the frequency of the current on the shield electrode, the current on the power supply electrode is changed with it. With the rotation of the electrode on the TBM face, the apparent resistivity and dispersion of the electrode at different positions can be obtained. As shown in Fig.3,

the anomalous body (high resistance) size is 4cmx4cmx4cm, which is located at the center axis of the palm face,9cm from the front of the palm, respectively, with alternating current of 0.1Hz,1Hz,5Hz,10Hz,20Hz. The visual resistivity cloud map and the dispersion cloud at four frequencies can be obtained. Figure. Results: The abnormal body can be detected by the apparent resistivity, and the location of the abnormal body can be obtained by calculating the dispersion rate.

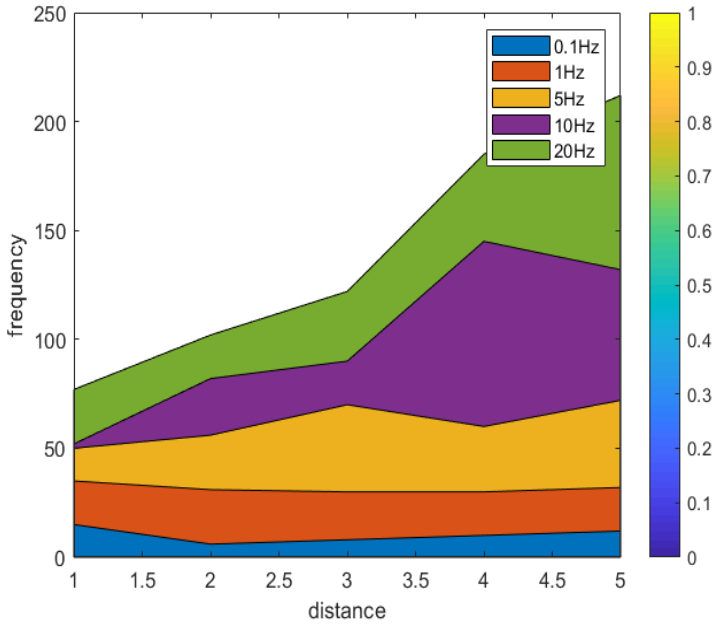

Figure 3. Resistivity and frequency distribution

4.2. Monitoring and Analysis of TBM Process

(1) Changing the distance between the abnormal body and the central axis

Change the distance between the anomaly body and the central axis of the TBM palm face to observe the detection effect. the size of the abnormal body (high resistance) was selected as 4 cm x 4 cm x 4 cm and the resistivity was 0.01 n m. the distance from the geometric center to the central axis of the abnormal body was changed for experiments, where s =0,3 cm,6 cm.As shown in Table 3 and Figure 4.the size of the abnormal body (low resistance) was selected as 4 cm x 4 cm x 2.5 cm and the resistivity was 1.0 x 10-6 n.m. the distance from the geometric center to the central axis of the abnormal body was changed for the experiment, where s =0,3 cm,6 cm. By changing the center of the abnormal body and the center of the palm

Table 3. Comparison of three options

Target delay(us)	Way 1	Way 2	Way 3
Target 1	751.0	421.9	579.8
Target 2	711.1	719.8	580.0
Target 3	724.3	737.1	693.1

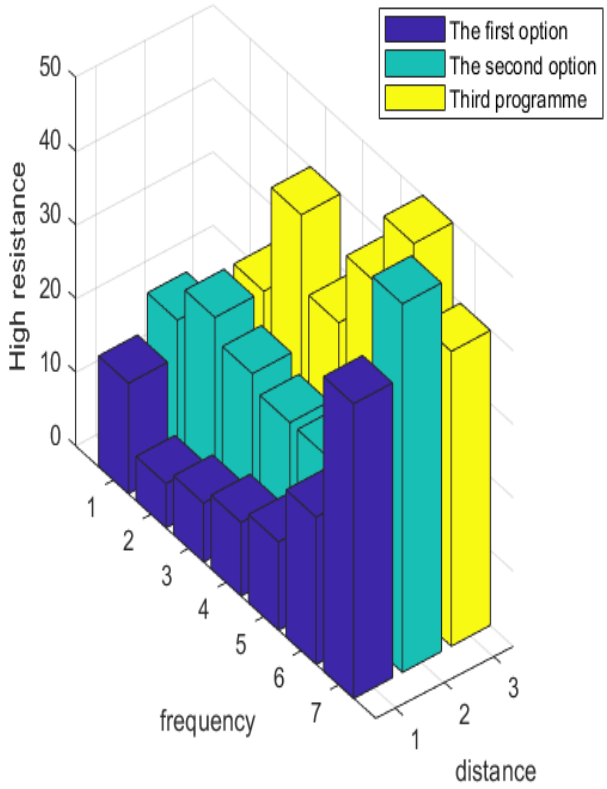

Figure 4. Changing the relationship between abnormal body and high resistance

(2) Changing the electrode distribution of TBM palm face

based on the distribution of the knife head on the face of the tbm is not completely uniform, two measuring electrode distribution modes are adopted, the isometric linear electrode distribution and the isometric interval 90 ° annular electrode distribution. As shown in Table 4 and Figure 5, the abnormal body (high resistance) size is 4cmx4cmx4cm, which is located at the central axis of the tbm palm face,9cm from the front of the palm, passing through the alternating current of 0.1 hz. by changing the electrode distribution on the palm face, it can be concluded that the iso-spaced linear electrode distribution is much more sensitive than the iso-spaced 90 ° annular electrode distribution. Analysis of results Because the experiment is homogeneous media, it is impossible to draw the conclusion of the detection effect in heterogeneous media for the time being.

Table 4. Comparison of three options

pair(km)	d_{12}(way 4)	d_{13}(way 5)	d_{23}(way 6)
Target 1	0	0.0186	0.0156
Target 2	0.272	0.0154	0.3046
Target 3	4.5670	3.9561	4.5752

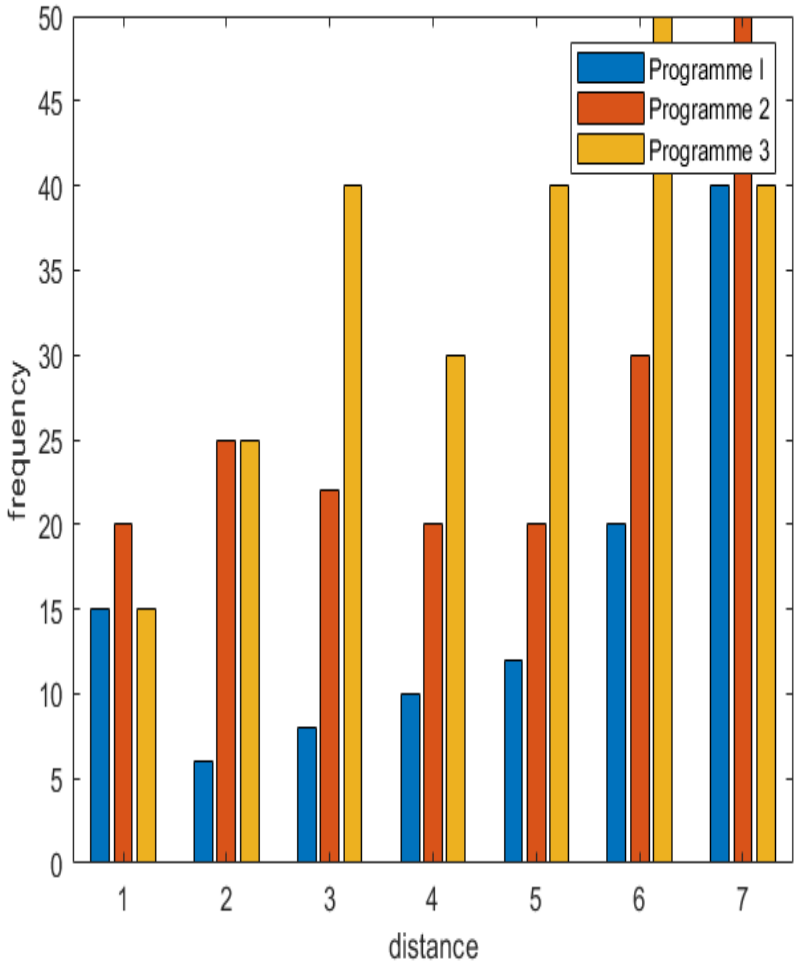

Figure 5. Changing the electrode distribution

5. Conclusion

Based on the safety monitoring system and method of TBM construction tunnel forward-to-cross-hole radar transmission imaging advance potential rock burst geological forecast, the design scheme and realization method of forward-to-three-dimensional multi-electrode on-line geological advance detector are proposed. First of all, this paper focuses on the numerical simulation, which makes the simulation results more accurate by optimizing the previous equations in two-dimensional and three-dimensional detection. Then, it focuses on the implementation of instrument function design and the technical optimization of each key software and hardware design to improve the stability, accuracy, real-time, ease of use, security and innovation of the system.

The theory of positive inversion in the field of geological advance detection has been deeply studied in the following three aspects, and the results have been obtained through the finite difference method, integral equation method, finite element method and boundary element method. Based on the characteristics of the frequency domain excitation polarization method and the need of scientific research and experiment in the project, this paper puts forward the development scheme of TBM construction tunnel forward three-dimensional real-time on-line advance detection system, which integrates the mature signal acquisition technology and real-time communication technology.

The circuit of avalanche pulses designed by TBM construction tunnel forward trans-hole radar transmission imaging and the depth of detection of the implanted ground penetrating radar depends largely on the amplitude of the avalanche pulses transmitted, and the pulses must not have tailing, waveform The stability is high, so the generation of high-voltage nanosecond narrow pulse signals is the key to the design.Using avalanche transistors, DC high-voltage power supplies, single-chip microcomputer control systems, and optocoupler modules, an avalanche pulse generation circuit is built. Increased output pulse amplitude (reachable). In this paper, forward trans-aperture radar is an effective geophysical detection instrument that uses high-frequency electromagnetic waves to determine the distribution of material in the medium. Combining with the specific application of advanced geological prediction of tunnels, this paper designs the launching and acquisition system of pulsed ground penetrating radar. A system synchronization control module with a single chip microcomputer as the core device is designed to generate a square wave signal with adjustable frequency, and provide a synchronous trigger signal for the avalanche pulse generation circuit and data acquisition module. A preliminary practical test of the launch and acquisition system was carried out. Experimental data show that the system can achieve the functions of avalanche pulse signal generation, synchronous transmission and reception, and real-time display. As a result, the safety detection factor has increased by about 80%. The experimental data show that the development of forward trans-hole radar transmission imaging is of great significance for the development of geophysical detection instruments, and it is of guiding significance for the establishment of a forward potential rock burst geological prediction safety monitoring system for TBM construction tunnel forward trans-hole radar transmission imaging.

Funding

This article is not supported by any foundation.

Data Availability

Data sharing is not applicable to this article as no new data were created or analysed in this study.

Conflict of Interest

The author states that this article has no conflict of interest.

References

[1] Xiaohui Yuan , Reem Atassi, Geological Landslide Disaster Monitoring Based on Wireless Network Technology, International Journal of Wireless and Ad Hoc Communication, 2021, Vol. 2, No. 1, pp: 21-32.https://doi.org/10.54216/IJWAC.020102

[2] Shan, P., & Lai, X. (2019) "Influence of CT Scanning Parameters on Rock and Soil Images", Journal of Visual Communication and Image Representation, 58(1), pp. 642-650. https://doi.org/10.1016/j.jvcir.2018.12.014

[3] Shan, P., & Lai, X. (2019) "Mesoscopic structure PFC similar to 2D model of soil rock mixture based on digital image", Journal of Visual Communication and Image Representation, 58, pp. 407-415. https://doi.org/10.1016/j.jvcir.2018.12.015

[4] Avila F R, Duarte L T, Biscainho L W P. On the sparsity-based identification and compensation of Hammerstein systems. IEEE Signal Processing Letters, 2017, 24(9): 1363-1367. https://doi.org/10.1109/LSP.2017.2720542

[5] *Liu D, Zhou Y, Jiao K. TBM construction process simulation and performance optimization. Transactions of Tianjin University, 2010, 16(3): 194-202. https://doi.org/10.1007/s12209-010-0035-0*

[6] *Wei M, Zhang N, Tong Y. Analysis of Abnormal Use of Cement Paste in Perfusion during Tunnel Construction using TBM. International Journal of Georesources and Environment-IJGE (formerly Int'l J of Geohazards and Environment), 2018, 4(2): 28-32. https://doi.org/10.15273/ijge.2018.02.005*

[7] *Wlodzimierz Greblicki, Miroslaw Pawlak. Hammerstein System Identification with the Nearest Neighbor Algorithm. IEEE Transactions on Information Theory, 2017, 4746 - 4757(63):8. https://doi.org/10.1109/TIT.2017.2694013*

[8] *Joemini Poudel, Lihong Wang, Mark Anastasio. Iterative image reconstruction algorithm for transcranial photoacoustic tomography applications. The Journal of the Acoustical Society of America, 2019, 145(3):1858-1858. https://doi.org/10.1121/1.5101707*

[9] *Manuel R. Arahal, Cristina Martin, Federico Barrero. Assessing Variable Sampling Time Controllers for Five-Phase Induction Motor Drives. IEEE Transactions on Industrial Electronics, 2019, PP(99):1-1.*

[10] *Gongyu H, Rong L, Cong J, et al. Risk Analysis and Evaluation of Long Slope Mining Construction by TBM Techniques. Chinese Journal of Underground Space and Engineering, 2016, 12(3): 831.*

[11] *Jin Guo, Haitao Liu. Hammerstein system identification with quantised inputs and quantised output observations.Iet Control Theory & Applications, 2017, 11(4):593-599. https://doi.org/10.1049/iet-cta.2016.1113*

[12] *Zhao Y, Liu Z. Research on TBM type selection risk for long draw water tunnel//IOP Conference Series: Materials Science and Engineering. IOP Publishing, 2019, 490(3): 032027. https://doi.org/10.1088/1757-899X/490/3/032027*

[13] *Mok W W S, Lo V K Y, Chau G T M, et al. Trenchless construction of Phase IIIA district cooling system (DCS) by TBM pipejacking and hand-dug tunnelling on Kai Tak Development: part I–design and construction considerations. HKIE Transactions, 2018, 25(1): 56-66. https://doi.org/10.1080/1023697X.2017.1413958*

[14] *Zhang H W, Zhu F, Han J, et al. Geological dynamic conditions and forecast technology for rock bursts. Journal of China Coal Society, 2016, 41(3): 545-551.*

[15] *Li C C, Mikula P, Simser B, et al. Discussions on rockburst and dynamic ground support in deep mines. Journal of Rock Mechanics and Geotechnical Engineering, 2019, 11(5): 1110-1118. https://doi.org/10.1016/j.jrmge.2019.06.001*

[16] *Kh. A. Khachatryan, Ts. É. Terdzhyan, T. G. Sardanyan. On the Solvability of One System of Nonlinear Hammerstein-Type Integral Equations on the Semiaxis. Ukrainian Mathematical Journal, 2017, 69(3):1287-1305. https://doi.org/10.1007/s11253-017-1431-6*

[17] *Kozyrev A, Konstantinov K. Development of an Express-Method to Control Damages in Underground Mining Excavations under Rockburst Hazardous Conditions. International Multidisciplinary Scientific GeoConference: SGEM: Surveying Geology & mining Ecology Management, 2017, 17(1.3): 253-259. https://doi.org/10.5593/sgem2017/13/S03.032*

[18] *Zhou J, Li X, Mitri H S. Classification of rockburst in underground projects: comparison of ten supervised learning methods. Journal of Computing in Civil Engineering, 2016, 30(5): 04016003. https://doi.org/10.1061/(ASCE)CP.1943-5487.0000553*

[19] *C. Zhu, Q. Li. Disparity Refinement Iterative Algorithm Based on Gradient Domain Guided Image Filtering. Tianjin Daxue Xuebao (Ziran Kexue yu Gongcheng Jishu Ban)/Journal of Tianjin University Science and Technology, 2018, 51(6):638-644.*

[20] *Lyu XZ, Zhao ZH, Wang XJ, Wang WM. Study on the Permeability of Weakly Cemented*

Sandstones," Geofluids, vol. 2019, Article ID 8310128, 14 pages, 2019. https://doi.org/10.1155/2019/8310128

[21] Shan, P., Lai, X., & Liu, X. (2019) "Correlational Analytical Characterization of Energy Dissipation-Liberation and Acoustic Emission during Coal and Rock Fracture Inducing by Underground Coal Excavation", Energies, 12(12), pp. 2382.https://doi.org/10.3390/en12122382.

[22] Kozyrev A A, Panin V I, Semenova I E, et al. Geodynamic Safety of Mining Operations under Rockburst-Hazardous Conditions in the Khibiny Apatite Deposits. Journal of Mining Science, 2018, 54(5): 734-743. https://doi.org/10.1134/S1062739118054832

[23] Erik Cuevas, Primitivo D áz, Omar Avalos. Nonlinear system identification based on ANFIS-Hammerstein model using Gravitational search algorithm. Applied Intelligence, 2017, 48(11):182-203. https://doi.org/10.1007/s10489-017-0969-1

[24] Guo J, Zhang W X, Zhao Y A. Multidimensional Cloud Model for Rockburst Prediction . Chinese Journal of Rock Mechanics and Engineering, 2018, 37(5): 1199-1206.

[25] Eyoh I, John R, Maere G D. Hybrid Learning for Interval Type-2 Intuitionistic Fuzzy Logic Systems as applied to Identification and Prediction Problems. IEEE Transactions on Fuzzy Systems,2018, PP(99):1-1. https://doi.org/10.1109/FUZZ-IEEE.2017.8015463

[26] Guruswamy A , Blum R . Ambiguity Optimization for Frequency-Hopping Waveforms in MIMO Radars With Arbitrary Antenna Separations. IEEE Signal Processing Letters, 2016, 23(9):1231-1235. https://doi.org/10.1109/LSP.2016.2569121

[27] Anastasios Deligiannis, Anastasia Panoui, Sangarapillai Lambotharan. Game-Theoretic Power Allocation and the Nash Equilibrium Analysis for a Multistatic MIMO Radar Network. IEEE Transactions on Signal Processing, 2017, PP(99):1-1. https://doi.org/10.1109/TSP.2017.2755591

[28] Junkun Yan, Hongwei Liu, Wenqiang Pu. Joint Beam Selection and Power Allocation for Multiple Target Tracking in Netted Colocated MIMO Radar System. IEEE Transactions on Signal Processing, 2016, PP(99):1-1.

[29] Yan J, Liu H, Pu W, et al. Joint beam selection and power allocation for multiple target tracking in netted colocated MIMO radar system. IEEE Transactions on Signal Processing, 2016, 64(24): 6417-6427. https://doi.org/10.1109/TSP.2016.2607147

[30] Ren D J, Shen S L, Arulrajah A, et al. Prediction model of TBM disc cutter wear during tunnelling in heterogeneous ground. Rock Mechanics and Rock Engineering, 2018, 51(11): 3599-3611. https://doi.org/10.1007/s00603-018-1549-3